Manufacturing large shafts by a novel flexible skew rolling process

Longfei Lin (colin0910@foxmail.com)
University of Science and Technology Beijing https://orcid.org/0000-0001-5513-3829
Baoyu Wang
University of Science and Technology Beijing
Jing Zhou
University of Science and Technology Beijing
Jinxia Shen
University of Science and Technology Beijing

Research Article

Keywords: Flexible skew rolling, Large shafts rolling, Forming defects, Forming precision, Feasibility study

Posted Date: May 13th, 2021

DOI: https://doi.org/10.21203/rs.3.rs-508796/v1

Version of Record: A version of this preprint was published at The International Journal of Advanced Manufacturing Technology on October 5th, 2021. See the published version at https://doi.org/10.1007/s00170-021-08079-y.

Manufacturing large shafts by a novel flexible skew rolling process

Longfei Lin[a], Baoyu Wang[a, b*], Jing Zhou[a, b], Jinxia Shen[a]

[a] School of Mechanical Engineering, University of Science and Technology Beijing, Beijing 100083, China

[b] Beijing Laboratory of Metallic Materials and Processing for Modern Transportation, Beijing 100083, China

*Corresponding author: Baoyu Wang

E-mail address: bywang@ustb.edu.cn

Tel: +86-010-82375671

Fax: +86-010-82375671

Postal address: No.30 Xueyuan Road, Haidian District, Beijing 100083, China

Abstract

When manufacturing large shafts with multi-specification and small-batch production, both the conventional forging and rolling process bring a high tooling cost due to heavy forging press or large-size specialized roller. In this study, a novel flexible skew rolling (FSR) process is proposed by adding degrees of freedom to the rollers as compared to the typical skew rolling process. Since each of the FSR rollers has three degrees of freedom (circle rotating, radial rotating and radial feeding), the FSR process can be divided into four stages: radial rolling, rollers inclining, skew rolling and rollers levelling. Therefore, the FSR process can produce various shafts with same rollers via programming different movements. To verify the feasibility of FSR process, a physical investigation corresponding with a numerical simulation for a single-step shaft is undertaken with a Φ80×390 mm C45 steel billet. According to the results from physical experiments and numerical simulations, the FSR formed shaft has a maximum deviation of 0.99 mm, and its microstructure and properties have been improved obviously. Moreover, although there is a tendency of center crack in FSR products as predicted by numerical results, both the transverse and longitudinal section of the physical shaft are free from central cracking. The major forming defects existed on the rolled shaft are knurled pockmarks, surface threads and side cavity, which are the typical defects of the conventional skew rolling and cross-wedge rolling and can be removed by machining. To the authors' knowledge, this novel process has a good combination of flexible production and less loading, which will be of great engineering significance to reduce the tooling cost in large shafts manufacturing.

Keywords: Flexible skew rolling, Large shafts rolling, Forming defects, Forming precision, Feasibility study

1. Introduction

Large shafts play an important role in large-elongated axial parts manufacturing and die-forging billets preforming, which are widely used on transportation vehicle, aerospace, construction machinery and other indutrial clusters, such as railway axles [1, 2], truck shafts [3], preform of turbine blade [4] and railway switch [5]. Up to now, these shafts are generally formed by forging process (open die forging [6, 7], radial forging [8, 9, 10]) and cross-wedge rolling (CWR) process [1,11,12]. Nevertheless, the forging process can manufacture various shafts by common rollers but needs a high forging force on account of its characteristic of overall deformation, which results in the heavy tonnage of forging equipment. Conversely, the cross-wedge rolling process can achieve less-loading forming by regional deformation but needs large-size specialized rollers. When manufacturing large shafts in multi-specification and small-batch production, both the forging and rolling process bring a high tooling cost due to the heavy loading press or the large-size specialized rollers.

In order to achieve flexible manufacturing, a process of axial feed rolling was early proposed and investigated [13,14], whose schematic diagram is shown in Fig. 1a. The workpiece is radially compressed via two rollers feeding radially and whereafter axially stretched under the chuck drawing. Therefore, the axial feed rolling process is a flexible production that same rollers can manufacture various multiple-step parts by different roller movements. However, because two rollers are paralleled with each other, the drawing force of the chuck is significant huge, especially in large shafts manufacturing.

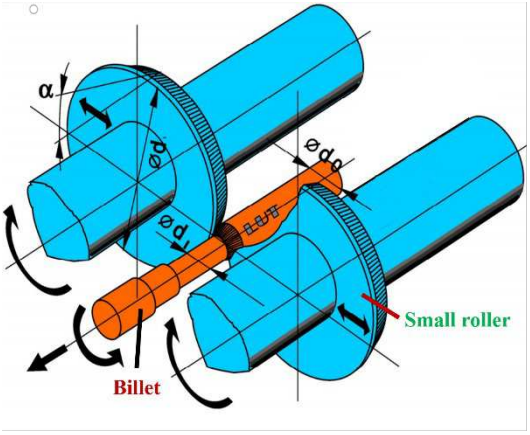

(a) axial feed rolling

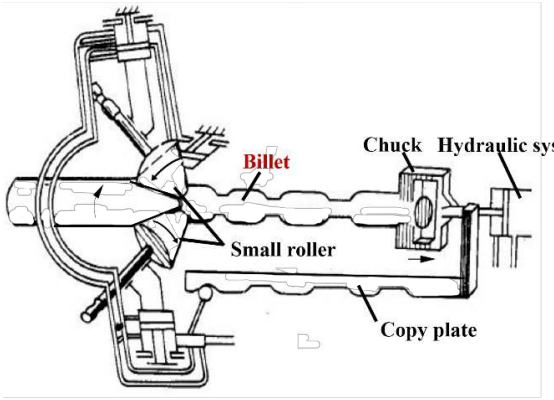

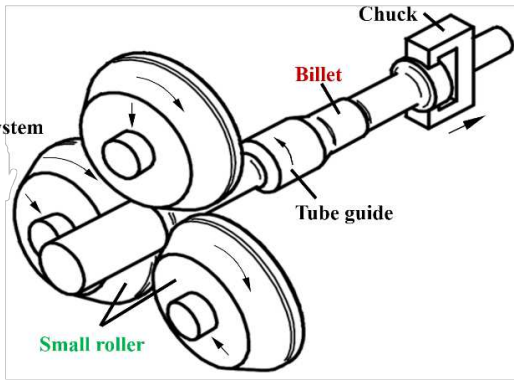

(b) copy skew rolling (c) CNC skew rolling

Fig. 1 The existing flexible rolling process for stepped shafts manufacturing

Another flexible rolling process is three-roller skew rolling method which can be divided into two types: copy skew rolling (Fig. 1b) and CNC skew rolling (Fig. 1c). Copy skew rolling is originated from the Soviet Union by Zerikov,1948 [15, 16], in which a copy plate is used to control the motions of tapered rollers. With the development of automatic control technology, Pater et al. [2, 17] used a CNC system to replace the copy unit and successfully accomplished the laboratory experiments of forming two rail axles in a CNC skew rolling mill. Significantly, due to the tapered rollers are inclined to each other, the rolling workpiece of copy skew rolling and CNC skew rolling can be automatically driven by the axial component of friction, so that the drawing force of the chuck can be significantly decreased.

Nevertheless, all these mentioned processes, whether in axial feed rolling, copy skew rolling or CNC skew rolling, a chuck is required to draw the workpiece in axial direction that may cause the limitations of :1) a considerable amount of chucking

allowance is indispensable that the material utilization is reduced; 2) the maximum length of the rolled shaft is limited by the chuck stroke of the mill. By far, all these flexible rolling methods are not seen in extensive application.

In this study, a novel flexible skew rolling (FSR) process is proposed by adding degrees of freedom to the rollers as compared to the typical skew rolling process. The aim of this presented paper is to verify the flexibility of this novel FSR process. Firstly, new type of FSR mill and FSR roller are designed, and their features are detailly introduced. Secondly, an FSR experiment of a Φ80 single-step shaft is performed to verify the feasibility of FSR process. Thirdly, a corresponding finite element (FE) numerical simulation are conducted to reveal the FSR deformation characteristic. At last, several types of physical experiments are performed to explore the FSR applications and reveal the FSR forming defects.

2. Flexible skew rolling (FSR) process

2.1 Novel process of flexible skew rolling

As shown in Fig. 2, a two-roller FSR process is invented by the authors [18]. Its rolling device mainly consists of two rollers and two tube guides. Each of two rollers has three degrees of freedom as circumferential rotating N_0, radial feeding V_0 and angle adjusting W_0. Two tube guides are respectively fixed on the sides of two rollers to restrict the movements of workpiece. By programming the motions (N_0, V_0, W_0) of two rollers in an automatic system, the FSR process can be divided into four stages (Fig. 2b): 1) radial rolling: two leveled rollers have the motions of N_0 and V_0, and then two rollers knife into the workpiece; 2) rollers inclining: two rollers only have the motion of W_0, and the skewing angle β is increased to target value; 3) skew rolling: two inclined rollers only have the motion of N_0, and the workpiece rotates circularly and moves axially; 4) rollers levelling: two rollers have the motions of V_0 and W_0, and then back to the original state.

Since the FSR process can be programmed into four stages, the FSR process can

flexibly form various shafts with same rollers. And according to the above descriptions, the FSR method has the following characteristics: 1) a drawing chuck is unessential because the workpiece can move axially under the action of axial friction; 2) the rolling equipment is relatively simple because only two rollers are needed; 3) an automated system is essential because the movements of two rollers is much complex and difficult to control.

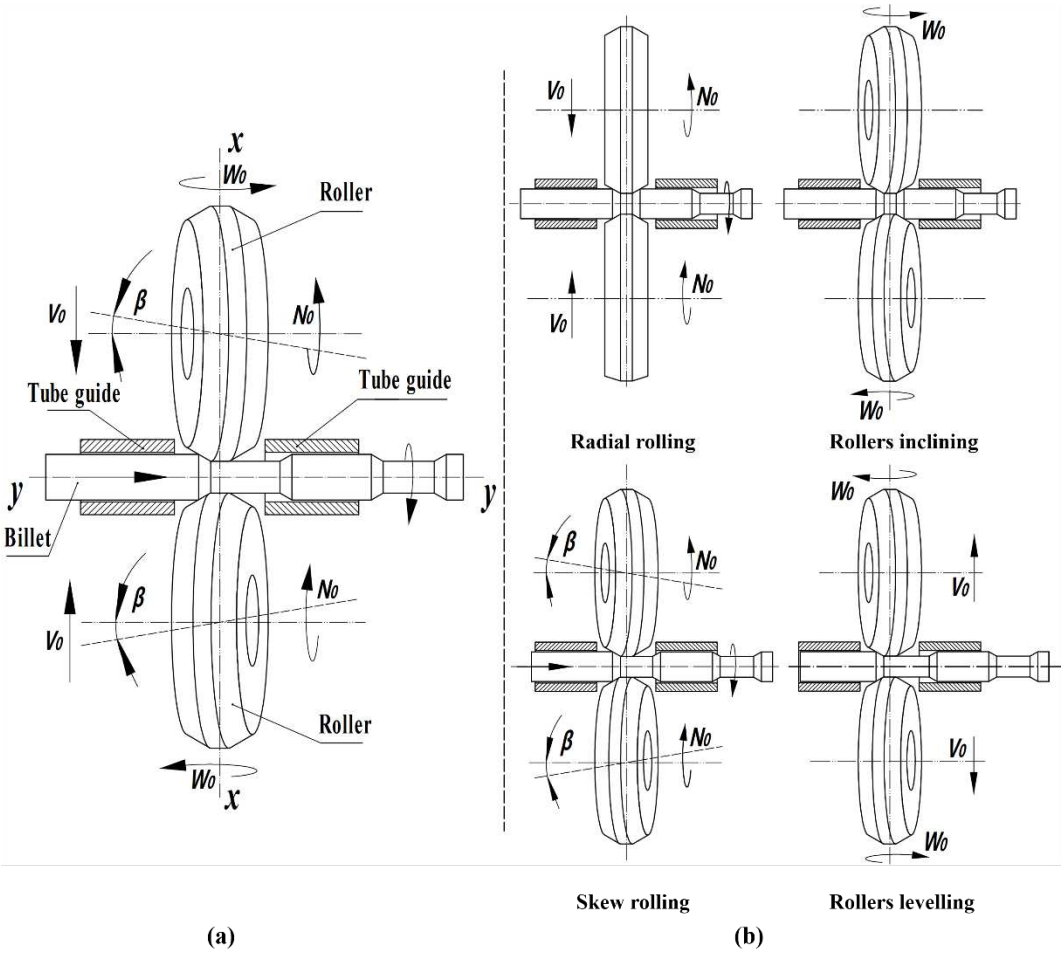

Fig. 2 Schematic illustration of flexible skew rolling (FSR): (a) process principle; (b) rolling stages [18]

2.2 New type of FSR mill and FSR roller

Because the FSR process is a new method, the design of FSR mill and roller is a critical job, and a number of attempts have been made. To meet the requirement of the FSR process, a laboratory FSR mill which has three degrees of freedom (N_0, V_0, W_0) is indispensable. Therefore, a new type of multi-freedom rolling mill has been invented and constructed [19]. Its 3D model is shown in Fig. 3. The physical mill is presented in

Fig. 4, and technical specifications are given in Table. 1. The FSR mill mainly consists of ten components: a base unit – 1, two tube guides – 2, two arm stands – 3, two angle adjusting systems – 4, two rollers – 5, two rotating systems – 6, a counter balance unit – 7, a radial feeding system – 8, a synchronous unit – 9, and a servo control system.

In the FSR mill, two rotating systems are correspondenly mounted under two arm stands and drive two rollers rotating around its axle. Two angle adjusting systems are fixed on the two arm stands to adjust the skewing angle, respectively. In order to make the radial feeding system synchronous, a synchronous unit worked by two matched gears is used to ensure two arm stands open or close together. What need to pay attention to is that, the overall dimension of this mill is 1.8 m×1.7 m×1.6 m and its total power is 70 kW, but the maximum billet diameter can up to 80 mm. We can have a conclusion that the FSR mill has a advantage of compactness structure.

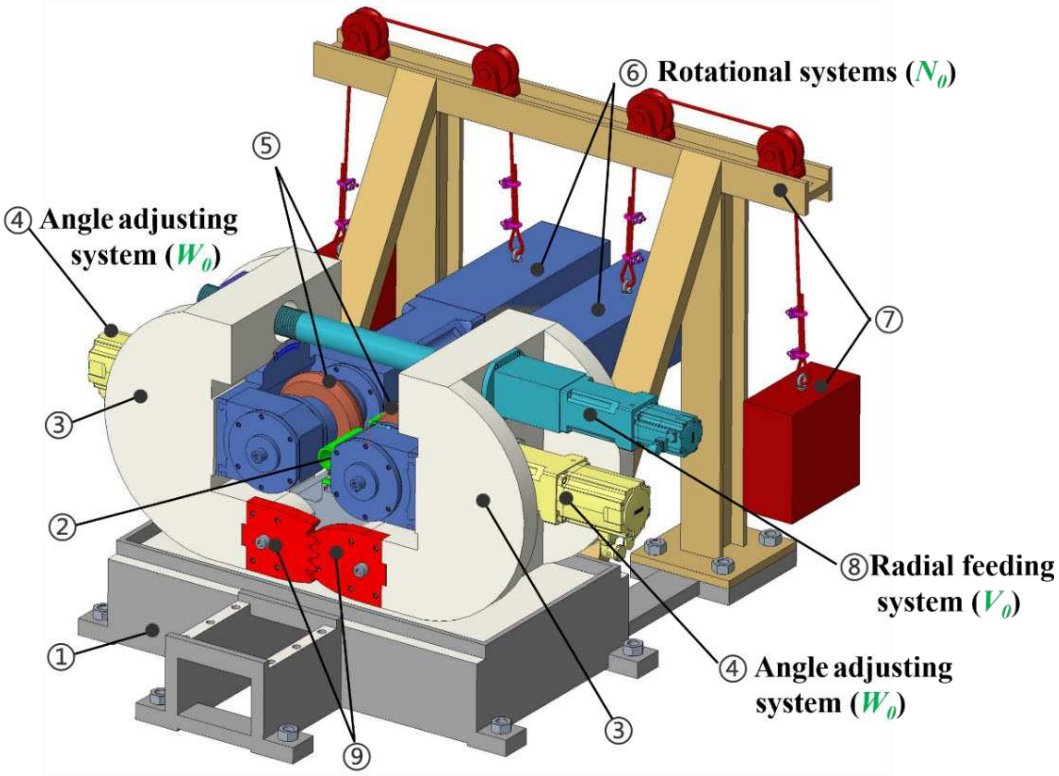

Fig. 3 3D geometrical model of FSR mill [19]

Fig. 4 A physical FSR mill was invented and constructed [19]

Table.1 Technical specifications of FSR mill

Parameter	Unit	Value
Main rotating motor power	kW	2×30
Main rotating speed	rpm	0~43
Radial feeding motor power	kW	3
Radial feeding speed	mm/s	1~5
Angle adjusting motor power	kW	2×2.3
Angle adjusting speed	°/s	1~10
Angle adjusting range	°	±12
Rolling center line range	mm	±0.15
Maximum roller diameter	mm	350
Maximum billet diameter	mm	80
Overall dimensions	m	1.8×1.7×1.6
Total power	kW	70
Total weight	ton	5

The FSR roller is inspired by the piercing roller [20] but has some developments because all the forming stages need to be considered and the workpiece needs to avoid crack. The FSR roller is shown in Fig. 5 and has a small size and a simple shape. It has a symmetrical structure of a sizing zone in the middle and two forming zones on both sides because the rolling force should be balanced in axis direction during the radial rolling stage. In addition, it is made by hot-die-material H13 and its hardness is measured as 53 HRC. Besides, the forming zone surface is knured by a 2 mm hatching knurling knife (CN standard, GB 6403.3) to improve the FSR rolling conditions. The geometric parameters of FSR rollers are: diameter D_0=340 mm, length L_0=120 mm, forming angle α =20 ° and sizing width L=25 mm.

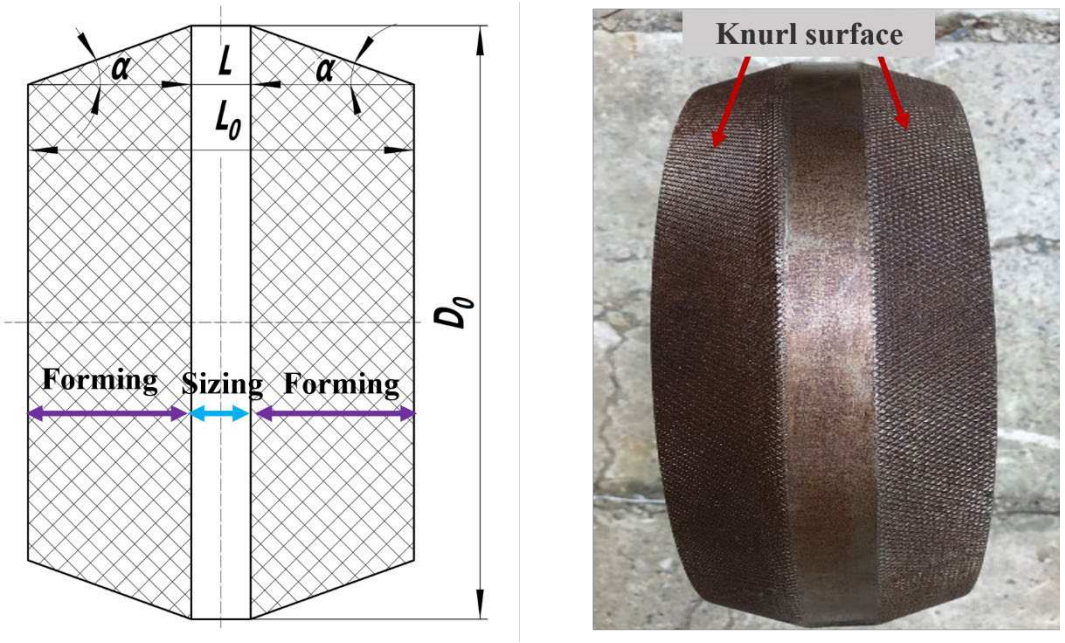

(a) (b)

Fig.5 New type of FSR roller: (a) geometric model; (b) physical graphics

3 Feasibility experiment of a Φ80 single-step shaft FSR rolling

3.1 FSR rolling experiment

To verify the feasibility of the FSR process, a physical feasibility experiment of a single-step shaft FSR rolling was undertaken with a Φ80×390 mm C45 steel billet. The physical experiment was performed at the University of Science and Technology Beijing, China. Because the rolled shaft only has one step, the FSR rolling process

simply includes three stages of radial rolling, rollers inclining and skew rolling. Although not all processes are included, two main forming stages (radial rolling, skew rolling) are totally covered. Therefore, it can be concluded that the feasibility experiment is reasonable.

The flow chart of rollers' movements is shown in Fig. 6. At the radial rolling stage, two leveled rollers rotate with a constant speed of N_0=30 rpm and feed radially with a speed of V_0=1.5 mm/s. After the radial rolling stage (10 seconds later), the gap between two rollers reaches the target value of 50 mm. During the rollers inclining stage, the inclining angles of two rollers are adjusted into a skewing angle of β=8 °. At the skew rolling stage, two rollers remain an inclined angle β=8 ° and rotate at the speed of N0=30 rpm, and the workpiece rotates circumferentially and moves axially under the frictional force.

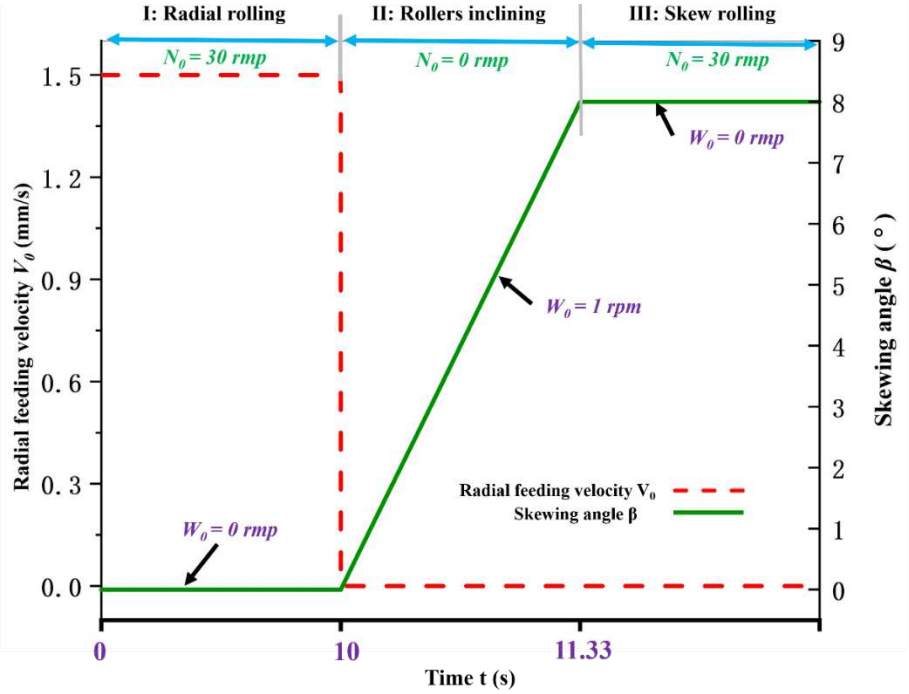

Fig. 6 Schematic diagrams of the movements of FSR rollers

Prior to the rolling, the billet was preheated to 1050℃ in an electric tube furnace and then immediately transferred to the FSR mill. As shown in Fig. 7, The workpiece was rolled stably during every stage. After FSR rolling, the product was removed and cooled in the air. The rolled shaft is shown in Fig. 8, whose cross-section shrinkage is exceeded 60%.

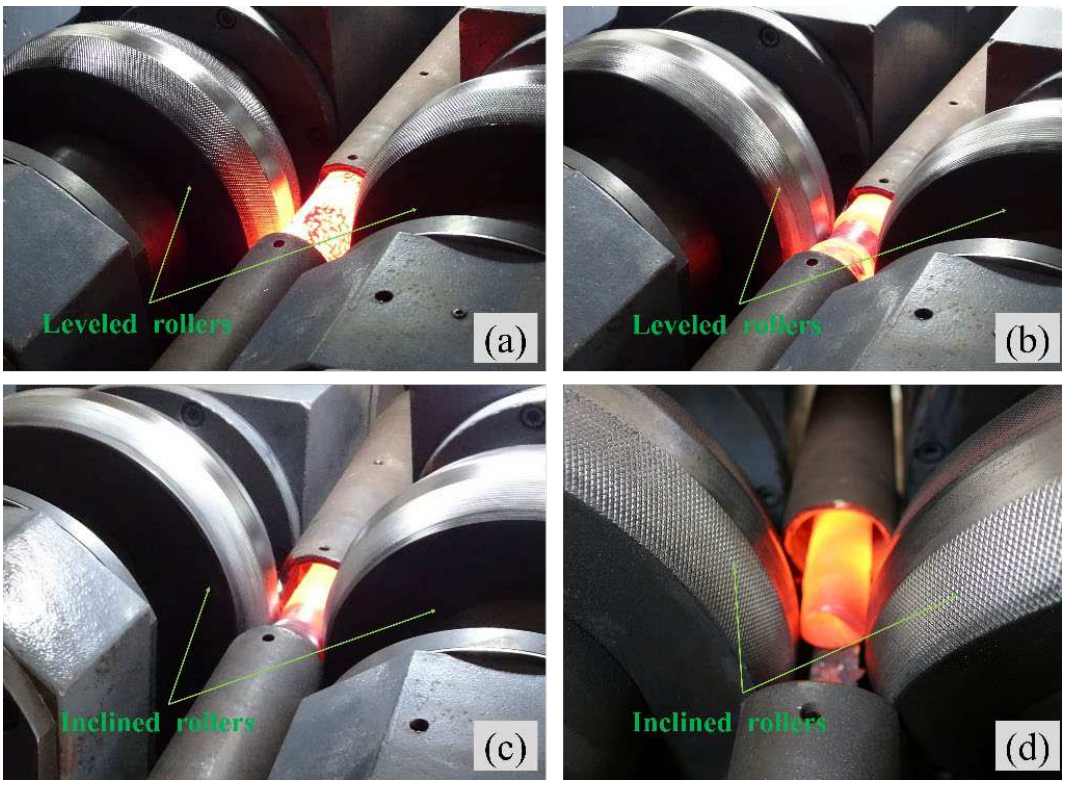

Fig. 7 FSR experiment for a Φ80 single-step shaft: (a) beginning of radial rolling stage; (b) during radial rolling stage; (c) during skew rolling stage; (d) ending

Fig. 8 A Φ80 mm single-step shaft was produced by FSR process: (a) just finished rolling; (b) after cooled at room temperature

By the feasibility test, the conclusions can be obtained: 1) the FSR process is feasible and optimistic; 2) the complex motions of rollers can be precisely regulated by FSR mill and the technical specifications of FSR mill are sufficient; 3) the temperature of the workpiece is relatively stable and still in the temperature range of hot deformation.

3.2 Results and discussion

3.3.1 Forming precision

The geometrical dimension of the FSR shaft was acquired by a high precision 3D scanner and then measured in Geomagic Quality software. As Fig. 9 shows, at radial rolling stage, the maximum and minimum diameter deviations of the FSR rolled shaft are +0.8 mm and -0.39 mm. Respectively, these of skew rolling stage are +0.99 mm and -0.35 mm. To do an analysis, because the workpiece is restricted by two tube guides, the rolled shaft does not bend easily, so that the diameter deviations mainly result from the surface threads.

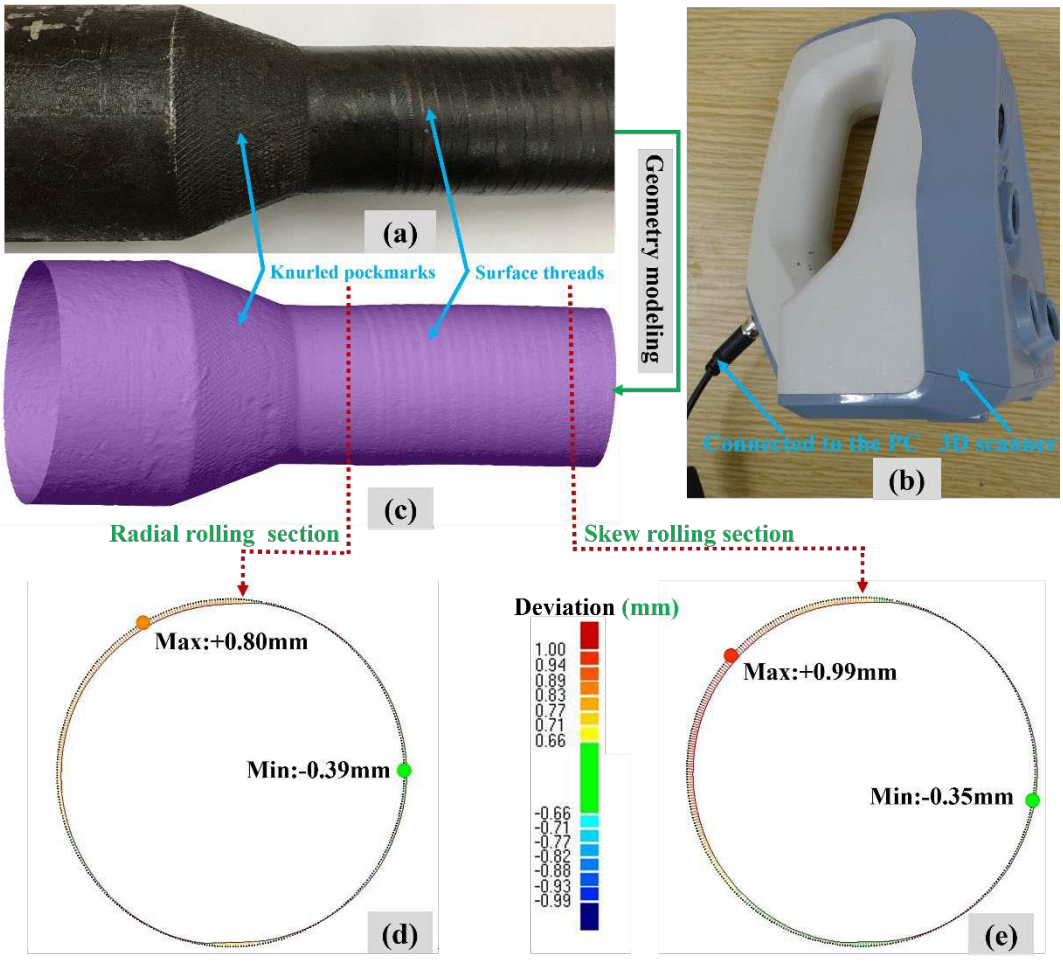

Fig. 9 The (c) geometric model of the (a) rolled shaft was modeled by a high precision (b) 3D scanner and their (d, e) dimensional deviations were measured.

There are some forming defects appeared on the rolled-shaft as shown in Fig.9a. The knurled pockmarks exist on the step surface because the rollers' surfaces were knurled by hatching knurling. In addition, the surface threads, which are formed at the stage of skew rolling, obviously present on the rolled rod. The main reason for these surface threads may be that the sizing length L is too short or the chamfering angle between the forming and sizing zone of the roller is unreasonable, thus futher research is necessary.

Another observed defect is the side cavity as shown in Fig.10b, which has a length of 36.8 mm and an angle of 61.2 °. It can be explained that the material of the outer sphere flows more rapid than that of the internal. This defect leads to the waste of the material, but does not affect the quality of products.

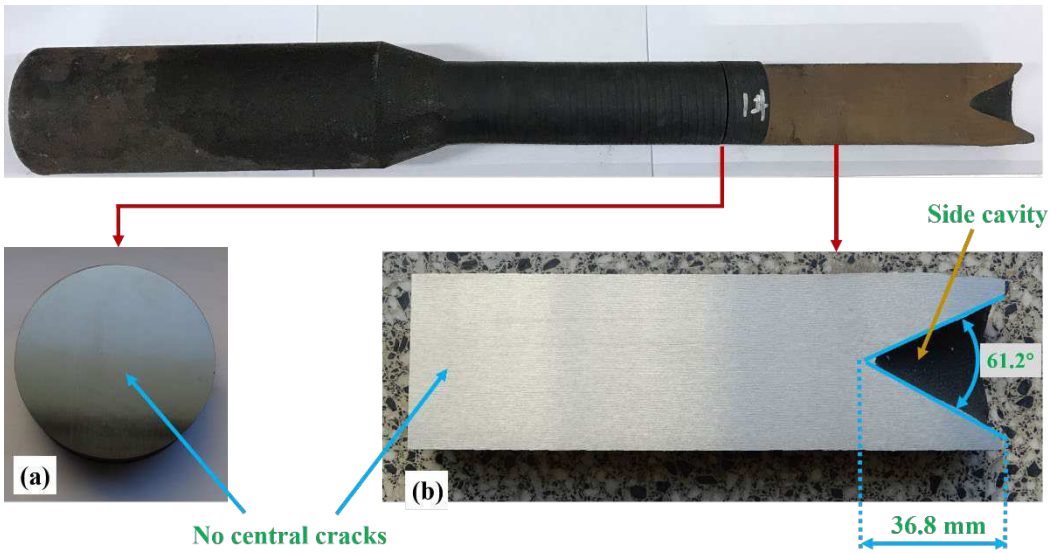

Fig. 10 FSR rolled shaft has the defect of side cavity and free from central cracks in macroscale: (a) transverse section; (b) longitudinal section

Actually, all these observed defects are the typical imperfections in skew rolling [2, 17, 21] and cross-wedge rolling [22, 23, 24] and can be removed in later precision machining, so do not affect the quality of produced shaft.

3.3.2 Central quality

Since the skew rolling stage of FSR process is much similar to the piercing process which has the trend of central cracking, we can estimate that, the central cracks, also

called the Mannesmann effect [25], may occur in the workpiece central and reduce the performance of formed parts.

For a observation in detail, both the transverse and longitudinal section of the FSR rolled shaft has been polished. As demonstrated in Fig. 10, it is clearly shown that the rolled shaft is free from any internal defects in the macroscale. Furthermore, its micro-morphology is observed by a 200 times magnification in the optical microscope. As shown in Fig. 11d, the magnified center is free from visible cracks or holes, which furtherly indicate the Φ80 mm single-step shaft has no center crack.

3.3.3 Microstructure evolution

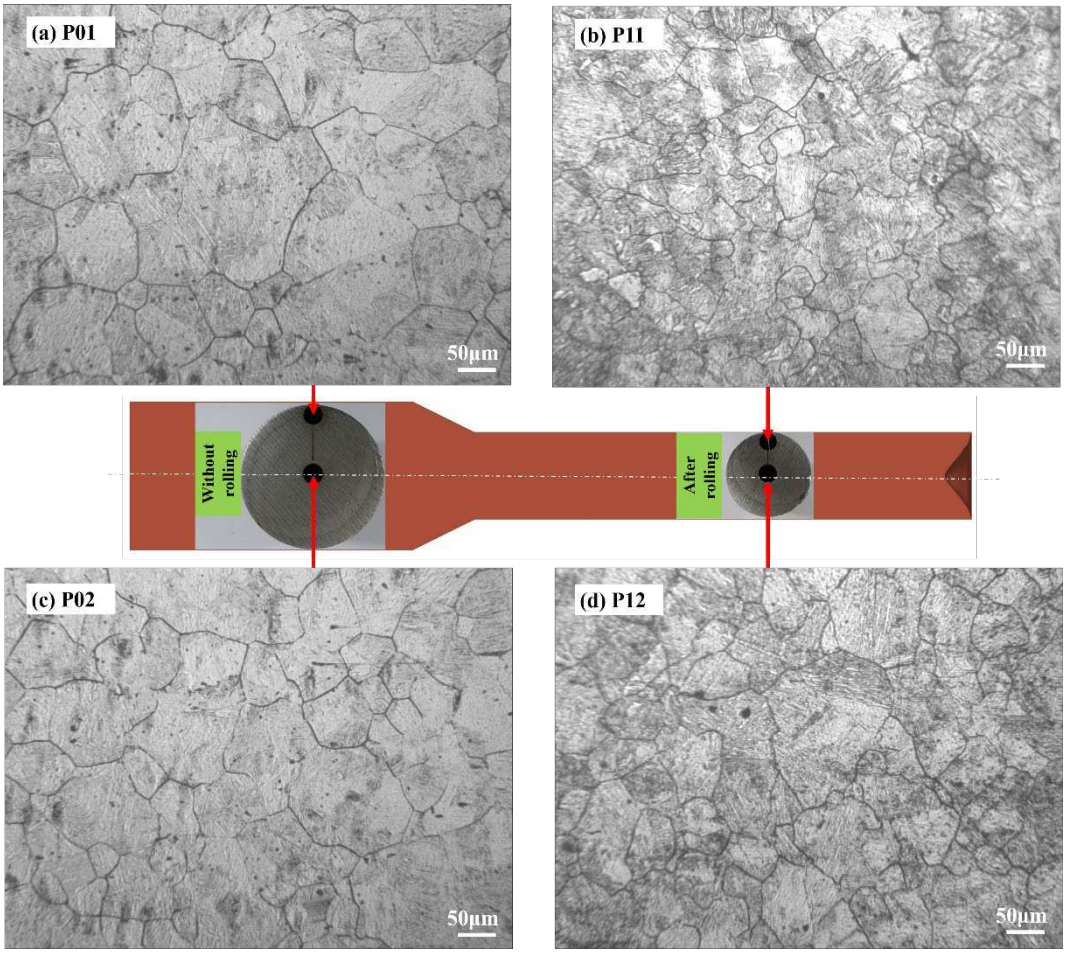

Fig. 11 Micromorphology of FSR rolled shaft at different locations (without visible cracks)

The microstructure evolution of the deformed metals is one of the most significant indicator to evaluate the mechanical propertie of FSR product. As shown in Fig. 11,

four samples named P01, P02, P11 and P12 were chosen from the outer and inner region of the unrolled and rolled rod. These samples were polished and etched, and their grains size and micro-morphology was obtained in a microscope with 200 times magnification.

As Fig. 11 shows, the grain sizes of rolled samples (P11,P12) are smaller than that of unrolled samples (P01,P02), it can be explained that the grains in outer and inner regions are refined by FSR rolling. Besides, the grains of the outer zone (P11) are obviously refined much greater than these of the inner (P11) because the outer materials have a much larger plastic deformation than central. All these observed results demonstrate that workpiece microstructures can be improved by the FSR process.

3.3.4 Mechanical properties

Testing the mechanical properties are essential to validate whether the FSR process is optimistic. Therefore, the ultimate tensile strength (UTS) and elongation were employed to characterize the mechanical properties. Four cylindrical samples were extracted from the outer and inner regions of unrolled and rolled rod and tested at room temperature with a drawing speed of 1 mm/min. The samples positions and tests results are detailly shown in Fig 12.

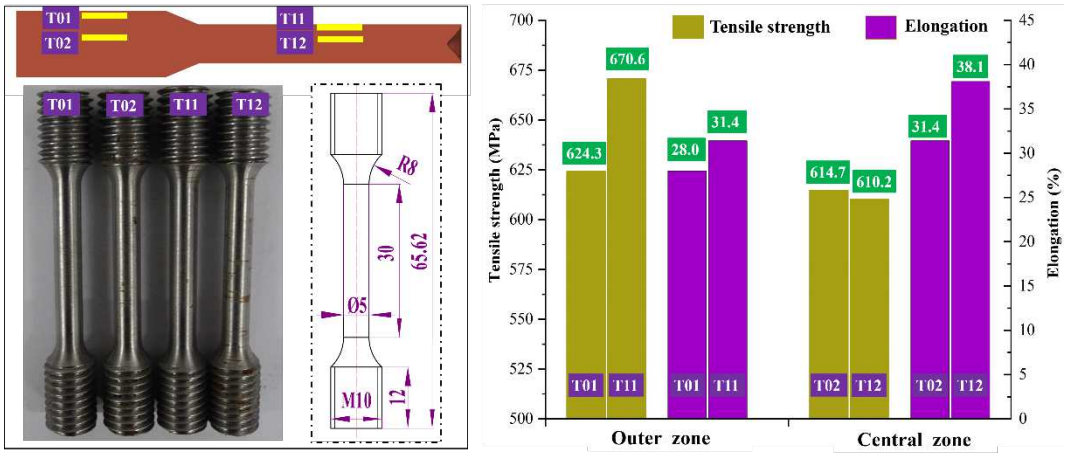

Fig. 12 Mechanical properties of FSR rolled shaft at different locations: (a) positions and dimensions of the tensiled samples; (b) the results of tension tests

In the outer zone, the UTS is significantly enhanced from 624.3 MPa to 670.6 MPa and the elongation is increased from 28.0% to 31.4%. However, in the center of the

shaft, the UTS is slightly reduced and the elongation is significantly improved. These performances can be explained that the outer materials have experienced a larger deformation that the outer grains are greater refined than the inner. As for the UTS slight decrease in the central zone, we can think that, the rolled bar has a smaller diameter and therefore the faster temperature drops cause the tensile strength increase. But in general, the overall mechanical properties of the whole shaft are improved after FSR deformation.

4 Finite element simulation of the feasibility experiment

4.1 FSR finite element modeling

The corresponding FSR FE projects were performed in Simufact.Forming software, which has been successfully employed in t numerical analysis of cross-wedge rolling process [26, 27] and skew rolling process [2, 28], and their FE results have a good agreement with experimental results. The FSR finite element model is based on the actual situations of the feasibility experiment, and their parameters are the same.

The material of the workpiece is C45. Its material data were taken from Simufact.Material. The properties (i.e., density, Young's modulus and Poisson's ratio) were set as default. The flow stress of C45 steel was defined by Eq. 1, in which σ_F is the flow stress (MPa), φ is the effective strain (-) and T is the temperature (°C):

$$\sigma_F = 2589.85e^{-0.003125T}\varphi^{(0.00004466T-0.10127)}e^{(-0.000027T+0.0008183)/\varphi}\dot{\varphi}^{(0.00015T-0.002749)} \quad (1)$$

The friction coefficients between tools and workpiece were modeled by Shear model (two rollers were 0.8, two tube guides were 0.2. [2] The temperature of tools (rollers, guides) was constantly maintained at 300 °C [2]. The initial temperature of workpiece was 1050 °C and the coefficient of heat transfer between tools and workpiece was 10 kW/m^{2}K [2]. Besides, the mesh of billet was created by ringmesh mesher, whose element size equals to 6 mm and will be automatically reconstruected if the effective strain increases by 0.4 [2]. The modeled FSR finite element model is displayed in Fig. 13.

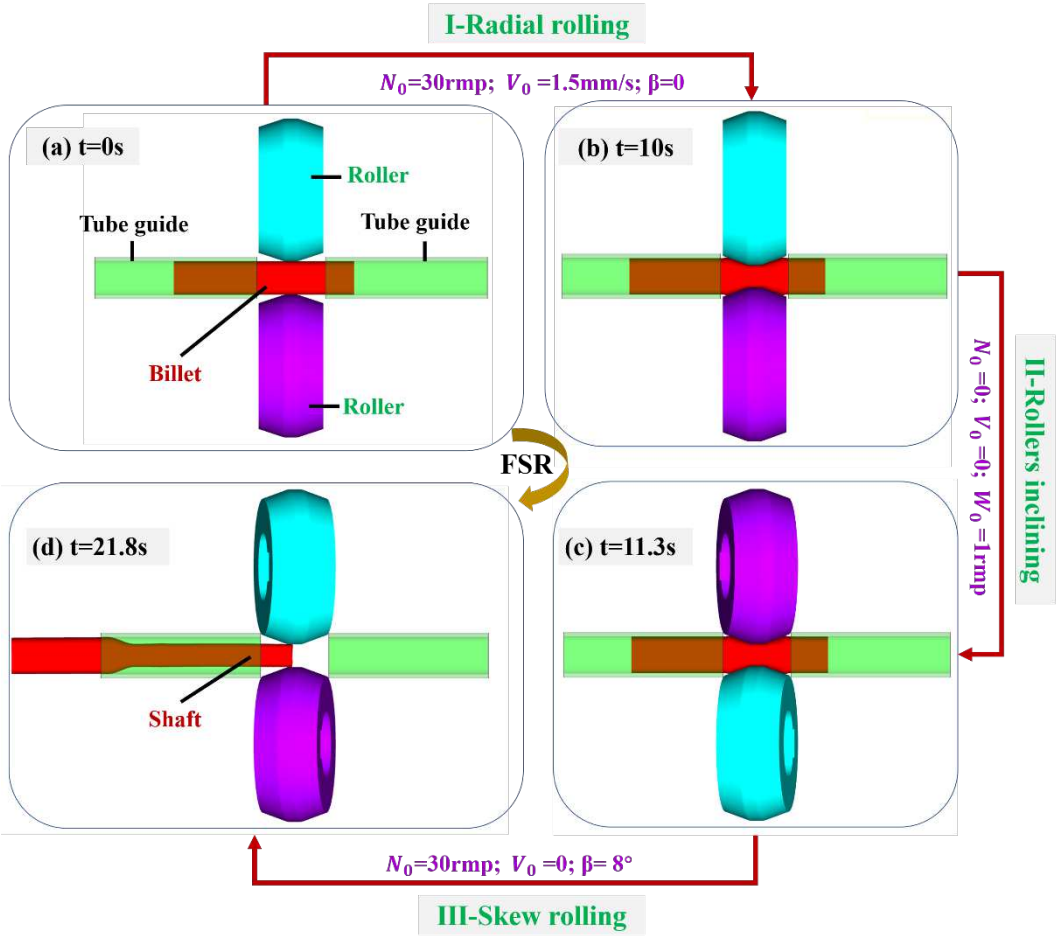

298

299 **Fig. 13** FSR finite element model of a Φ80mm single-step shaft

300 4.2 FSR finite element model validating

301 The FSR FE model was validated by a method of comparing the final geometry
302 parameters of the rolled shaft between physical and FE results which was used in the
303 study of Zhou [29]. The geometric parameters of FE model and experimentation were
304 measured in the Geomagic Quality software. The comparison results include total
305 length L, side cavity angle γ, minimum diameter D_{min} and maximum diameter D_{max} of
306 the rolled bar.

307 The geometry comparison is shown in Table.2. The maximum relative deviation
308 (relative to physical result) of four geometric parameters is side cavity angle γ with a
309 value equal to 2.1%, and all these deviations within the 10% range, so that the FSR
310 finite element model can be considered reliable.

311

Table 2 Geometry comparison between physical and FE results

Parameters	L	D_{min}	D_{max}	γ
Deviations	0.28%	0.40%	0.39%	2.1%
Results	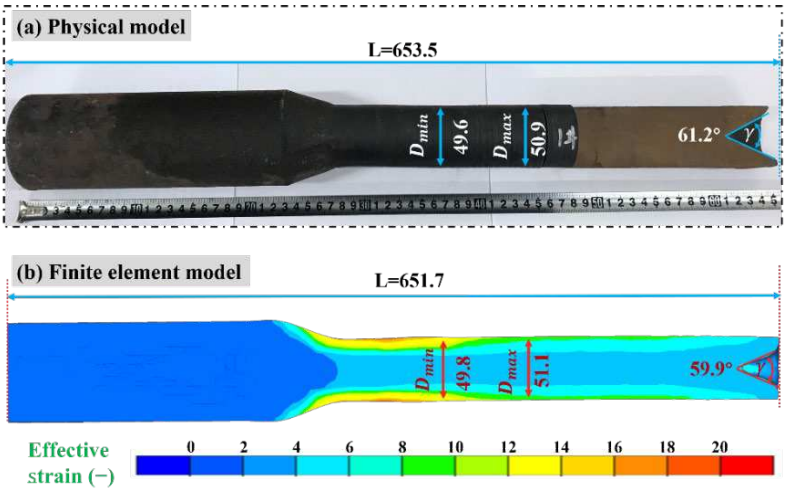			

4.3 Results and discussion

4.3.1 Deformation characteristics

In the application of finite element software, the FSR deformation process can be extracted from FE simulation results. As shown in Fig. 14, at the stage of rollers inclining, the workpiece has a slight deformation. Therefore, it can be obtained that the main forming stages of FSR process are radial rolling stage and skew rolling stage. At the radial rolling stage, the workpiece is bit into a groove and deformed on two sides. The metals in contacting zone are radially compressed and axially elongated, and the axial movements of workpiece are at a same speed V_{R1} but with opposite directions. During the skew rolling stage, two rollers contact with the workpiece only in one side, and the rolling workpiece radially rotates and axially feeds automatically under the function of friction component because two rollers are inclined.

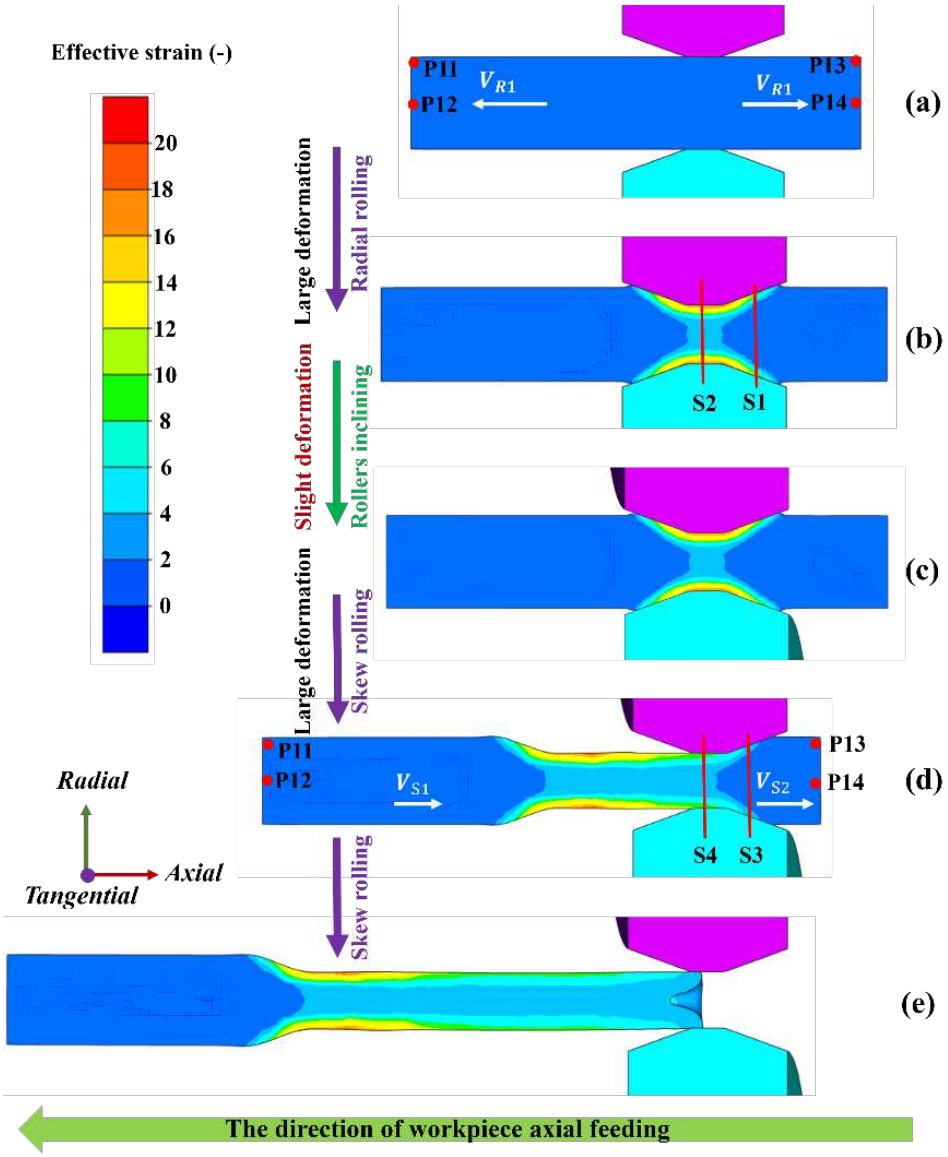

Fig. 14 Rolling stages and strain distributions of the Φ80 mm single-step FSR shaft: (a) beginning; (b) ending of radial rolling / beginning of rollers inclining; (c) ending of rollers inclining / beginning of skew rolling; (d) middle of skew rolling; (e) ending

In fact, the deformation characteristics of FSR have some similarities to the CWR process which was described in the study of Xu [30]. The workpiece is radially knifed primarily and then stretched axially. We can think that, the radial rolling stage is similar to the knifing stage in CWR, while the skew rolling stage is similar to the stretching stage of CWR.

Since the equal-diameter bar of the rolled shaft is formed by skew rolling, another feature of the FSR deformation is that the major forming stage of the FSR forming is skew rolling stage. To be specific, the shaft is formed by the roller' forming zone and

sized by the roller' sizing zone. Therefore, we can come to a conclusion that the skewing angle β, forming angle α and sizing length L are extremely important to FSR process.

4.3.2 Central quality of workpiece

According to the experiences of skew rolling and cross-wedge rolling, the Mannesmann hole [25] may occur in the center of FSR workpiece and cause the failure of products. To obtain the evolutions of stress and ductile damage, four transverse sections named S1, S2, S3, S4 were selected to do a analyze. As signed in Fig. 14, S1 and S3 are the forming sections of radial rolling and skew rolling while S2 and S4 are the sections after rolling.

Figure 15 shows the distribution of FSR stress. At the radial rolling stage, the central materials are exerted two tension stress and one compression stress. More specifically, the radial stress is a compressive stress which gradually reduces from the surface to the center, and the tangential or axial stress is a tensile stress which locally concentrated in the workpiece center.

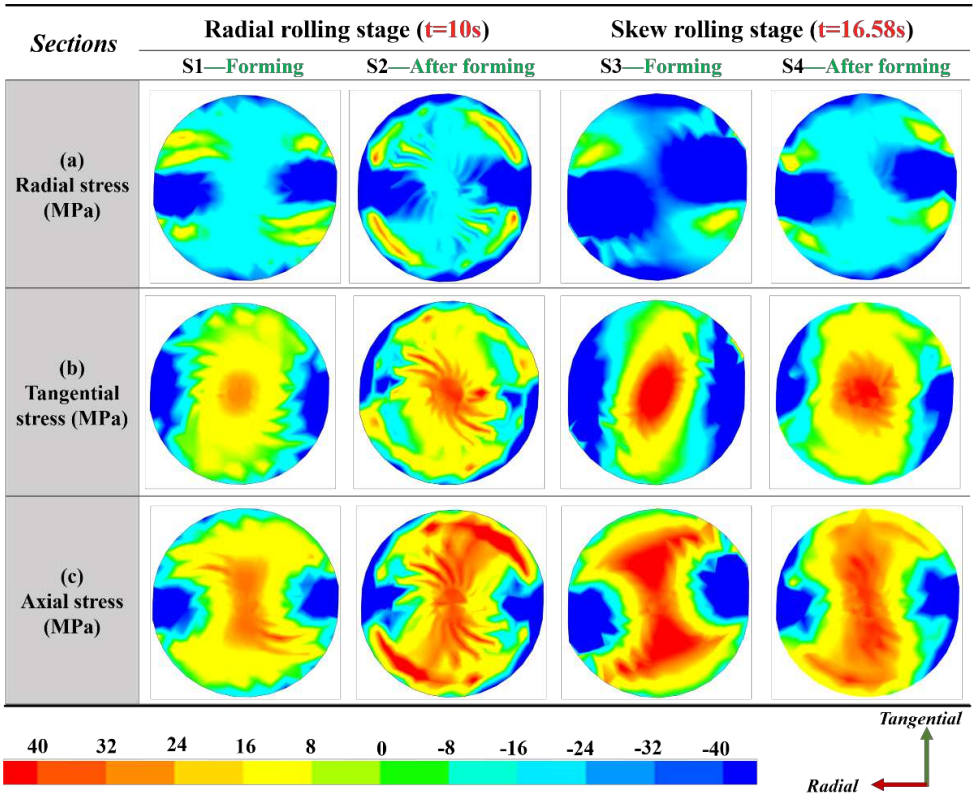

Fig. 15 Stress distributions of FSR workpiece

During the skew rolling stage, the stress distribution characteristics are identical to the rolling stage that two tension stress and one compression stress exist in the central region. Compared to the radial rolling stage, the tangential tension stress and axial tension stress at skew rolling stage become bigger. The radial stress of the central zone is compressive with a relatively small value of approximate 20 MPa while tangential stress and axial stress are tensile with a relatively larger value exceed 40MPa. Since the stress distribution state of the center is tension in two orientations and one compression in one orientation which may causes the generation of micro-cracks, it can be concluded that the FSR process is susceptible to central crack.

Three typical damage models were used to predict the damage state in FSR process (Fig. 16). Cockcroft and Latham [31] considered that the damage value is equal to the ratio of maximal principal stress and effective stress. Oyane [32] proposed a ductile damage model which based on the characteristics of porous materials. Ayada et al. [33] held an opinion that ductile fracture only depends on the history of stress triaxiality.

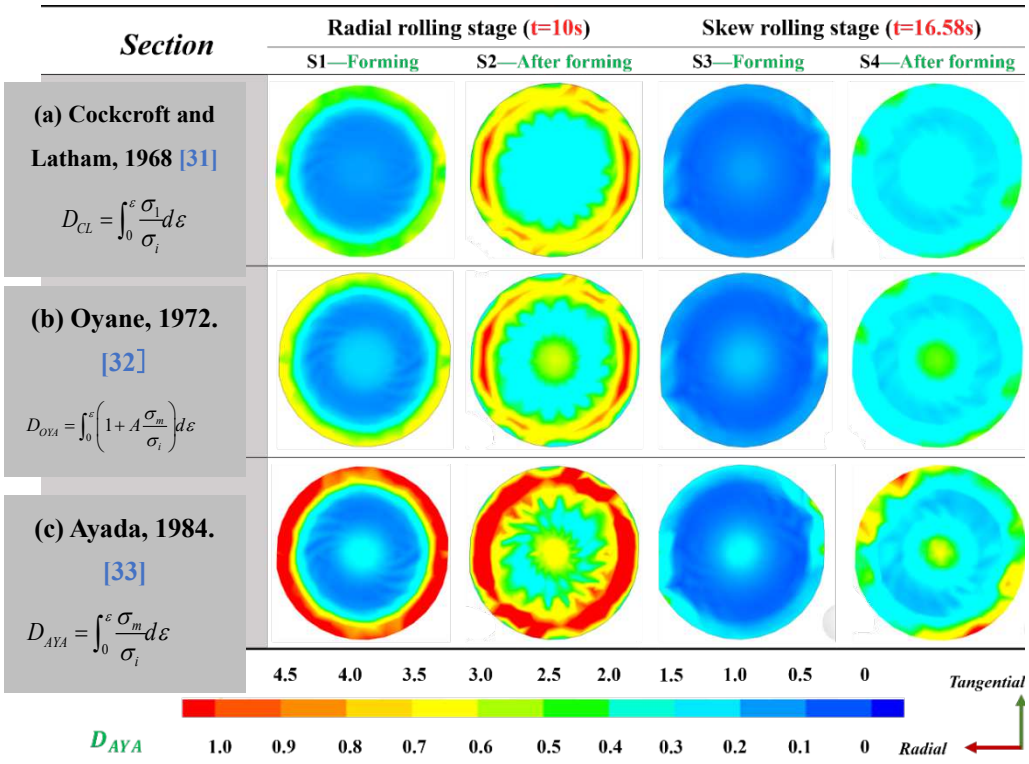

Fig.16 Ductile damages of FSR workpiece: (a) Cockcroft and Latham [31]; (b) Oyane [32]; (c) Ayada [33], in which ε is effective strain, σ_1 is maximal principal stress, σ_i is effective stress, σ_1 is mean stress, A is a material coefficient (0.424) [34]

The ductile damages are calculated by the functions demonstrated in Fig. 16. Furthermore, in order to get the damage distribution from FE software, the user subroutine of Simufact.Forming was employed to implement these criteria, so the damage values can unconditionally update at every increment and visible analyzed in the postprocessor. As shown in Fig. 16, it can be obviously observed that the ductile damages of three criterions have some commons: 1) there are damage concentrations in the central region; 2) the ductile damages increase evidently at the stage radial rolling and skew rolling. These findings are consistent with the stress distribution conditions analyzed above, so it can be obtained that the FSR process has a trend of central cracking. In addition, although it is shown that there are also some large ductile damages in the outer region, it can be explained that the outer workpiece undergoes a large tensile stress.

However, it is noteworthy that the damage distribution can reveal the trend of central crack which may be occured under unreasonable parameters, but it cannot be judged that the simulation results are inconsistent with the experiment because the predicted damage value may not reach the fracture threshold value.

4.3.3 Axial feeding velocity

The axial feeding velocity of the workpiece directly determines the FSR production efficiency. Four tracking points (P11, P12，P13 and P14) are selected, and their axial velocities are demonstrated in Fig. 22. During the radial rolling stage, the axial feeding velocities of the workpiece from inlet to outlet side have the same value V_{R1} but in different directions. However, at the skew rolling stage, its value in inlet (V_{S1}) and outlet side (V_{S2}) are not the same. Quantitative analysis reveals that the axial moving speed of radial rolling stage is relatively small with a value of approximately 2mm/s. At the skew rolling stage, the value of axial moving speed has a larger number with an average value of about 28.5 mm/s in outlet side.

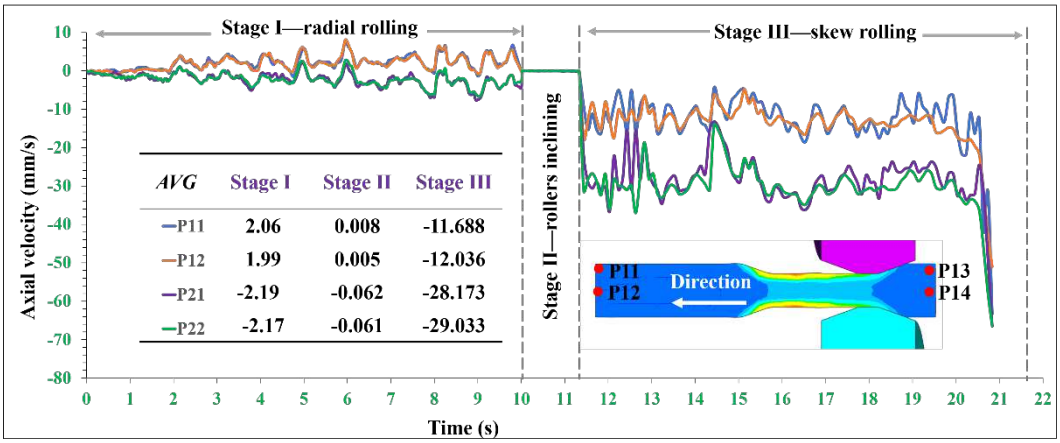

Fig.17 Rolling speed and duration of FSR process

Actually, the axial feeding velocity of workpiece is affected by rotating speed N_0, forming angle α and skewing angle β. The rotating speed N_0 of this study is only 30 rpm, which is relatively low in skew rolling. However, the total rolling time is as short as 20 seconds. It can be concluded that the production of FSR is efficient.

4.3.4 Temperature distribution

The temperature distribution is investigated as shown in Fig. 18. It can be observed that the temperature of the workpiece is relatively stable. Meanwhile, it can be noticed that the temperature increases locally at the working area because the deformation and friction cause the heat generation. The surface of billet have a temperature drop, which can be explained that it undergoes a local cooling because the heat is dissipated to the air, but fortunately the temperature is still in the range of the hot deformation. What's more, since the temperature drops slowly and the rolling time is short that the workpiece temperature can be stabilized within a hot formability range, so the billet of FSR process need to be heated only once, which obviously reduce energy consumption.

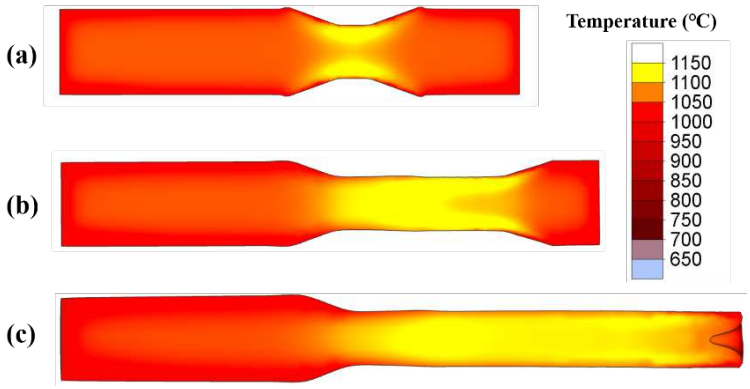

Fig. 18 Temperature distributions of FSR workpiece: (a) ending of radial rolling stage (b) middle of skew rolling stage; (c) ending of skew rolling stage

4.3.5 Rolling force and rotating torque

The force parameters of rolling force and rotating torque are the basic data in equipment designment. As shown in Fig. 19, at the roller leveling stage, both the rolling force and rotating torque are very small, which further verify that the workpiece have a very slight deformation at this stage. However, at the forming stages (radial rolling stage and skew rolling stage), the rolling force and torque change correspondingly with relatively large values. Concretely, the rolling force differs little with a value about 150 kN. The rotation torque of the spindle motor varies greatly with a maximum value of approximate to 8700 Nm.

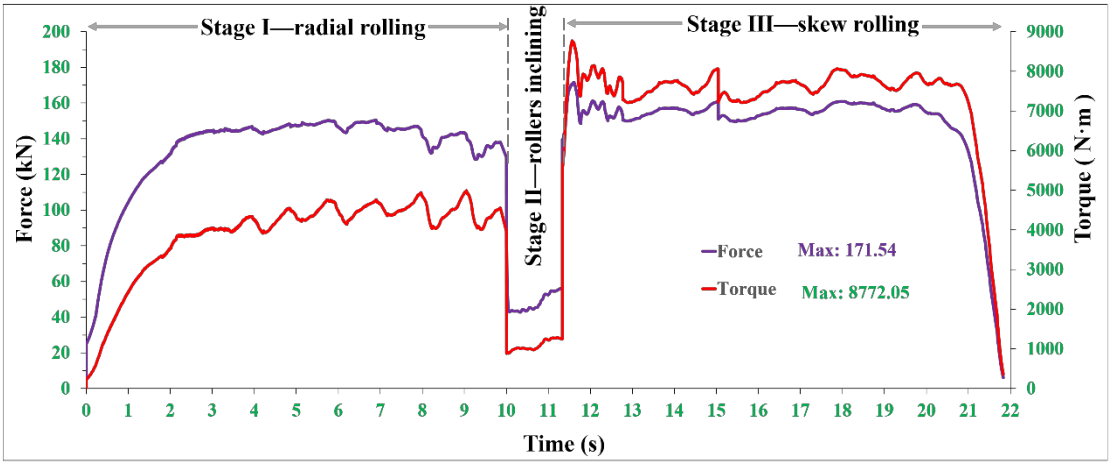

Fig. 19 Rolling force and rotating torque of FSR mill

5 Application exploration

The above studies in this paper are based on a simple single-step shaft, but in fact the shapes of large shafts are changed variously. In order to explore the industrial applications, some physical experiments were carried out with different rollers to form various parts in the laboratory (Fig. 20). Because it can form different shafts by same rollers, these flexible experiments were conducted conveniently. There are two types of parts were produced: bars and step-shafts.

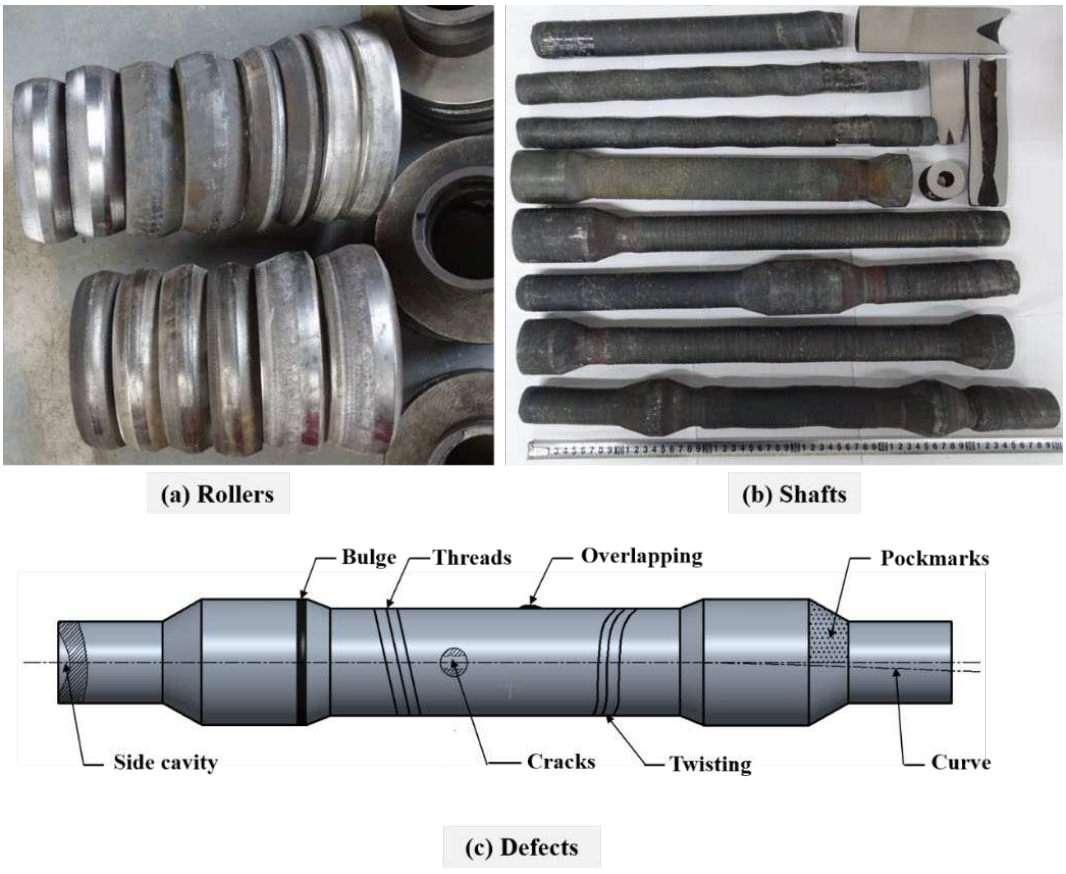

Fig. 20 Exploratory experiments were accomplished through (a) different rollers and (b) shafts, and (c) FSR defects appear on the rolled shafts

As shown in Fig. 20a, the rollers have different geometries including symmetric rollers and tapered rollers (the tapered roller is generally used in copy skew rolling and CNC Skew rolling, as Fig. 1 show), and their parameters of sizing length L and forming angle α are also varied in different values. By carrying out the experiments, we found that the tapered roller is not suitable for the FSR process because the step bulge appeared in the radial rolling process due to asymmetric deformation. Besides, the roller

material and its heat treatment process are very important because the FSR roller stands high temperature, rapid rotation, and large rolling force. Moreover, the small forming angle α and large skewing angle β are favorable for billet feeding, but conversely it will increase the possibility of central cracking. The big sizing length L can directly reduce the surface threads, but will result in the increase of the rolling force. Therefore, a process window needs to be established in further studies.

The shaft with multiple steps was rolled and displayed in Fig. 20b. Attention should be paid, there are some forming defects that evidently appeared in the formed products. These defects are summarized in Fig. 20c, in which side cavity, surface threads, pockmarks and central cracks are the most noteworthy limitations. These defects limit the application of the FSR process and need to be solved in future studies.

6 Conclusions

·A novel method named flexible skew rolling (FSR) has been proposed and verified through physical experiment and FE simulation. The FSR process can be expected to produce large shafts in small equipment and form various shafts with same rollers.

·The FSR rolled shaft has a maximum deviation of 0.99 mm. Although there is a tendency of center cracks as FE results predict, the physical shaft is free from internal cracks and its microstructure and mechanical properties are generally improved.

·The FSR forming defects are summarized by an exploratory experiment of forming various shafts with different rollers, of which the most noteworthy limitations are central cracks, surface threads and side cavity, so that the generation mechanisms and optimization methods for FSR defects need to be investigated in further studies.

·The deformation characteristics of the FSR process are similar to cross-wedge rolling that the workpiece is radially compressed initially and then stretched axially, but the movements of FSR rollers are much similar to piercing rolling that the inclined rollers drive the workpiece rotates circularly and moves axially.

·FSR process has an optimistic efficiency with an axial feeding velocity of 28.5

mm/s in outlet side, which is beneficial to keep the temperature relatively stable, so the workpiece needs to be heated only once.

·The loading of the FSR process is relatively light that the maximum radial rolling force is about 150 kN and the maximum rotation torque is about 8700 Nm of a Φ80 mm shaft.

Compliance with Ethical Standards

Acknowledgments

This work is supported by the National Key R&D Program of China (Grant No. 2018YFB1307900). This work is funded by the National Natural Science Foundation of China (Grant No. 51875036).

Conflict of interest statement

We declare that we have no financial and personal relationships with other people or organizations that can inappropriately influence our work, there is no professional or other personal interest of any nature or kind in any product, service and/or company that could be construed as influencing the position presented in, or the review of, the manuscript entitled.

Ethical approval

This article does not contain any studies with human participants or animals performed by any of the authors.

Informed consent

All the authors listed have approved the manuscript that is enclosed.

Authors' contributions

Longfei Lin: Software, Investigation, Validation, Methodology, Writing-Original Draft. Baoyu Wang: Project administration, Supervision, Funding acquisition. Jing Zhou: Methodology, Writing-Reviewing & Editing. Jinxia Shen: Data Curation, Writing-Reviewing & Editing.

Availability of data and materials

The datasets generated and/or analysed during the current study are available from

the corresponding author on reasonable request.

Consent to participate

Applicable.

Consent to publish

Applicable.

References

[1] Ji H, Liu J, Fu X, Tang X, Wang B, Huang X (2017) Finite element analysis and experiment on multi-wedge cross wedge rolling for asymmetric stepped shaft of C45. Journal of Central South University 24: 854-860. https://doi.org/10.1007/s11771-017-3487-8

[2] Pater Z, Tomczak J, Lis K, Bulzak T, Shu X (2020) Forming of rail car axles in a CNC skew rolling mill. Arch Civ Mech Eng 20:69. https://doi.org/10.1007/s43452-020-00075-5

[3] Yang C, Hu Z (2016) Research on the ovality of hollow shafts in cross wedge rolling with mandrel. Int J Adv Manuf Tech 83:67-76. https://doi.org/10.1007/s00170-015-7478-3

[4] Li J, Wang B, Fang S, Chen P (2020) A new process chain combining cross-wedge rolling and isothermal forging for the forming of titanium alloy turbine blades. Int J Adv Manuf Tech 108:1827-1838. https://doi.org/10.1007/s00170-020-05451-2

[5] Zwanenburg W (2006) Degradation processes of switches & crossings. Institution of Engineering & Technology International Conference on Railway Condition Monitoring IET :115-119. https://doi.org/10.1049/ic:20060054

[6] Lee Y, Lee S, Tyne C, Joo B, Moon Y (2011) Internal void closure during the forging of large cast ingots using a simulation approach. J Mater Process Tech 211(6):1136-1145. https://doi.org/10.1016/j.jmatprotec.2011.01.017

[7] Du S, Li Y, Song J (2015) Optimization of forging process parameters and anvil design for railway axle during high-speed forging. Asme International Mechanical Engineering Congress & Exposition. https://doi.org/10.1115/IMECE2015-50695

[8] Ghaei A, Movahhedy M, Taheri K (2005) Study of the effects of die geometry on deformation in the radial forging process. J Mater Process Tech 170(1-2):156-163. https://doi.org/10.1016/j.jmatprotec.2005.04.100

[9] Zou J, Ma L, Jia W, Le Q, Qin G,Yuan Y (2021) Microstructural and mechanical response of ZK60 magnesium alloy subjected to radial forging. J Mater Sci Technol 83:228-238. https://doi.org/10.1016/j.jmst.2020.11.080

[10] Romanenko V, Stepanov P, Kriskovich S (2018) Production of hollow railroad

axles by screw piercing and radial forging. Metallurgist 61:873-877. https://doi.org/10.1007/s11015-018-0579-0

[11] Peng W, Zheng S, Chiu Y, Shu X, Zhan L 2016 Multi-wedge cross wedge rolling process of 42CrMo4 large and long hollow shaft. Rare Metal Materials and Engineering 45(4):836-842. https://doi.org/10.1016/S1875-5372(16)30084-4

[12] Pater Z (2020) Numerical analysis of the cross-wedge rolling process of a railway axle. Mechanik(2):18-21. https://doi.org/10.17814/mechanik.2020.2.6

[13] Houska M (1999) Experiment and finite-element analysis of axial feed bar rolling (AVQ). The 6th International Conference on Technology of Plasticity:1523-1538.

[14] Xu C, Liu G, Ren G, Shen Z, Ma C, Ren W (2007) Finite element analysis of axial feed bar rolling. Acta Metallurgica Sinica 20(006):463-468. https://doi.org/10.1016/S1006-7191(08)60011-3

[15] Li C, Su X, Hu Z (2006) Status and research of axle forming methods for railway shafts. Metallurgical Equipment 6:5-8. In Chinese. https://doi.org/10.3969/j.issn.1001-1269.2006.06.002

[16] Hu Z, Zhang K, Wang B, Shu X, Yang C (2004) Technology and simulation of part rolling by cross wedge rolling. Metallurgical Industry Press, Beijing. In Chinese,

[17] Pater Z, Tomczak J, Bulzak T (2020) Problems of forming stepped axles and shafts in a 3-roller skew rolling mill. J Mater Res Technol 9(5):10434-10446. https://doi.org/10.1016/j.jmrt.2020.07.062

[18] Wang B, Lin L., J. Liu, C. Yang (2021) Device and method for forming shaft part by two-roller flexible skew rolling. European Patent No. 3733322.

[19] Wang B, Lin L, Wang S. Yang C, Liu S, Zhang H (2021) Flexible skew rolling mill with dual-rotatable-shafts. United State Patent No. 16/906729.

[20] Pater Z, Kazanecki J (2006) Thermo-mechanical analysis of piercing plug loads in the skew rolling process of thick-walled tube shell. Metallurgy and foundry engineering 32(1):31. https://doi.org/10.7494/mafe.2006.32.1.31

[21] Gamin Y, Akopyan T, Koshmin A, Dolbachev A, Goncharuk A (2020) Microstructure evolution and property analysis of commercial pure Al alloy processed by radial-shear rolling. Arch Civ Mech Eng 20:143. https://doi.org/10.1007/s43452-020-00143-w

[22] Shen J, Wang B, Zhou J, Lin L, Feng P, Investigation on the inner hole spiral-groove of cross wedge rolling of hollow shafts with mandrel. Int J Adv Manuf Technol 110:1773–1787. https://doi.org/10.1007/s00170-020-05801-0

[23] Shu X, Shi J, Chen Ji, Yang H (2021) Effect of process parameters on surface quality of shafts parts formed by warm cross wedge rolling. Int J Adv Manuf Tech

113:2819-2813. https://doi.org/10.1007/s00170-021-06784-2

[24] Feng P, Yang C, Wang B, et al (2021) Formability and microstructure of TC4 titanium alloy hollow shafts formed by cross-wedge rolling with a mandrel. Int J Adv Manuf Tech 114:365–377. https://doi.org/10.1007/s00170-021-06635-0

[25] Ghiotti A, Fanini S, Bruschi S, Bariani P (2009) Modelling of the Mannesmann effect. CIRP Annals - Manufacturing Technology, 58(1):255-258. https://doi.org/10.1016/j.cirp.2009.03.099

[26] Tofil A, Tomczak J, Bulzak T (2015) Numerical and experimental study on producing aluminium alloy 6061 shafts by cross wedge rolling using a universal rolling mill. Arch Metall Mater 60(2):801-807. https://doi.org/10.1515/amm-2015-0210

[27] Pater Z, Tomczak J, Bulzak T (2016) Cross-wedge rolling of driving shaft from titanium alloy Ti6Al4V. Key Eng Mat 687:125–32. https://doi.org/10.4028/www.scientific.net/KEM.687.125

[28] Lis K, Wójcik U, Pater Z (2016) Numerical analysis of a skew rolling process for producing a crankshaft preform. Open Engineering 6:581-584. https://doi.org/10.1515/eng-2016-0087

[29] Zhou X, Shao Z, Zhang C, Sun F, Zhou W, Hua L, Jiang J, Wang L (2020) The study of central cracking mechanism and criterion in cross wedge rolling. Int J Mach Tool Manu 159:103647. https://doi.org/10.1016/j.ijmachtools.2020.103647

[30] Huang X, Wang B, Zhou J, Ji H, Mu Y, Li J (2017) Comparative study of warm and hot cross-wedge rolling: numerical simulation and experimental trial. Int J Adv Manuf Technol 92:3541–3551. https://doi.org/10.1007/s00170-017-0399-6

[31] Zhou J, Yu Y, Zeng Q (2014) Analysis and experimental studies of internal voids in multi-wedge cross wedge rolling stepped shaft. Int J Adv Manuf Technol 72:1559-1566. https://doi.org/10.1007/s00170-014-5768-9

[32] Novella M, Ghiotti A, Bruschi S, Bariani P (2015) Ductile damage modeling at elevated temperature applied to the cross wedge rolling of AA6082-T6 bars. J Mater Process Tech 222:259-267. https://doi.org/10.1016/j.jmatprotec.2015.01.030

[33] Ayada M, Higashino T, Mori K (1984) Central bursting in extrusion of inhomogeneous materials. In Proceedings of the First International Conference on Technology of Plasticity:553-558.

[34] Pater Z, Tomczak J, Bulzak T, Wójcik U, Walczuk P (2019) Assessment of ductile fracture criteria with respect to their application in the modeling of cross wedge rolling. J Mater Process Tech 278:116501. https://doi.org/10.1016/j.jmatprotec.2019.116501